The Coulomb effect on a low-energy structure in above-threshold ionization spectra induced by mid-infrared laser pulses*

Lin Zhi-Yang(林志阳)[a)e)], Wu Ming-Yan(吴明艳)[a)e)], Quan Wei(全 威)[a)], Liu Xiao-Jun(柳晓军)[a)†], Chen Jing(陈 京)[b)c)‡], and Cheng Ya(程 亚)[d)]

[a)] State Key Laboratory of Magnetic Resonance and Atomic and Molecular Physics, Wuhan Institute of Physics and Mathematics, Chinese Academy of Sciences, Wuhan 430071, China

[b)] HEDPS, Center for Applied Physics and Technology, Peking University, Beijing 100871, China

[c)] Institute of Applied Physics and Computational Mathematics, Beijing 100088, China

[d)] State Key Laboratory of High Field Laser Physics, Shanghai Institute of Optics and Fine Mechanics, Chinese Academy of Sciences, Shanghai 201800, China

[e)] University of Chinese Academy of Sciences, Beijing 100049, China

(Received 16 April 2013; revised manuscript received 7 May 2013; published online 10 December 2013)

We investigate the low-energy structure (LES) in the above-threshold ionization spectrum at a mid-infrared laser wavelength with a semiclassical model. Using a softened Coulomb potential (CP) and changing the softening parameter, we show that though the very low-energy structure (VLES) and high low-energy structure (HLES) are both due to the interaction between the ionic CP and the electron, the two structures have different physical mechanisms: the VLES can be attributed to the electron–ion Coulomb interaction at a rather small distance and the HLES is more likely to be ascribed to the electron–ion Coulomb interaction at a large distance.

Keywords: low-energy structure, above-threshold ionization, electron–ion Coulomb interaction

PACS: 32.80.Rm, 42.50.Hz, 32.80.Wr **DOI:** 10.1088/1674-1056/23/2/023201

1. Introduction

Above-threshold ionization (ATI), which was first discovered by Agostini *et al.*,[1] has greatly contributed to the understanding of atomic and molecular dynamics in intense laser fields for the past 30 years.[2–5] ATI can be classified as either multiphoton ionization (MPI) or tunneling ionization depending on the Keldysh parameter $\gamma = \sqrt{I_p/2U_p}$ based on Keldysh's theoretical framework,[6] where I_p is the ionization potential and $U_p = I/4\omega^2 \propto I \times \lambda^2$ is the ponderomotive energy[7] of an electron in a laser field with frequency ω (wavelength λ) and intensity I. The tunneling ionization prevails in the regime corresponding to a high intensity and long wavelength, i.e., $\gamma < 1$. In this regime, the simple-man model[8–11] successfully describes several fundamental features in the ATI photoelectron energy spectrum, such as the formation of a high-electron-energy plateau,[12] the sidelobes in angular distributions (AD) of electrons[13] and a λ^2 scaling of the $10U_p$ cutoff, confirmed in recent experiments with mid-infrared wavelength laser pulses.[14]

However, the low-energy momentum distribution[15,16] of recoiling ions evidently deviates from this simple-man model, which reveals a significant influence of the Coulomb potential (CP) of the parent ion on low-energy electron dynamics.[15,17,18] More recently, a peculiar peak-like low-energy structure (LES) with an electron energy of above 1 eV, or a high-energy low-energy structure (HLES), which becomes most pronounced at mid-infrared wavelengths, e.g., 2000 nm, was observed by Blaga *et al.*[19] and Quan *et al.*[20] The HLES is at variance with the model and witnesses an "ionization surprise".[21] It is found that the peak position and width of the HLES primarily depend on the laser parameters. Moreover, the HLES is absent for circularly polarized laser pulses and its angular distribution (AD) becomes narrow at long wavelengths.[22,23] In Ref. [19], a full numerical solution of the time-dependent Schrödinger equation (TDSE) is able to reproduce the HLES but no physical explanation is identified; the HLES remains absent in the simulation based on the well-known Keldysh–Faisal–Reiss (KFR) model.[6,24,25] On the other hand, a semiclassical model has been used to investigate the HLES and the CP is considered to be responsible for its physical origin.[20] Liu and Hatsagortsyan[26,27] performed similar simulations and demonstrated that the HLES originates from an interplay between the multiple forward rescatterings and the distortion of trajectories by the CP near the core. Furthermore, the HLES is considered to be from the trajectories of electrons moving away from the detector with a reverse initial transverse momentum.[28,29] More recently, the HLES is also reproduced by the second-order term in the S-matrix expansion, taking into account the long-range Coulomb potential.[30]

*Project supported by the National Natural Science Foundation of China (Grant Nos. 10925420, 11074026, 11174330, and 11274050) and the National Basic Research Program of China (Grant Nos. 2011CB808102 and 2013CB922201).

†Corresponding author. E-mail: xjliu@wipm.ac.cn

‡Corresponding author. E-mail: chen_jing@iapcm.ac.cn

© 2014 Chinese Physical Society and IOP Publishing Ltd

In particular, besides the HLES, the sharp hump structure with energies well below 1 eV, or a very low-energy structure (VLES), was also reported by Quan *et al.*[20] In contrast to the HLES, the VLES exhibits an independence of laser parameters, such as intensity and wavelength, which eluded experimental observation in Ref. [19] and many theoretical studies.[26–30] More recently, the VLES, corresponding to the double-hump structure in longitudinal momentum distribution, was confirmed experimentally by Wu *et al.*[31] using the sophisticated cold target recoil-ion momentum spectroscopy (COLTRIMS) and the effect of the long-range CP on the photoelectron with a very low energy upon its return has been suggested to be responsible for this VLES. Moreover, a mechanism of energy bunching was introduced by Kästner *et al.*,[32] who suggested that the LES is composed of a series of peaks, in which the lowest ones are believed to correspond to the VLES.[31] Meanwhile, multiple peaks in the LES were also investigated by Lemell *et al.*,[33] while the experimental observability of the VLES may be limited by the deficiency of measurements in some experiments.[34] However, so far, most studies have focused on HLES and very little work has been done on VLES. Considering a pivotal role of VLES in a full understanding of dynamics of the low-energy electrons in the ATI process, a comprehensive investigation of the underlying physical mechanism behind VLES, especially the role of CP in the production of VLES, is still demanded.

In this paper, we investigate the mechanism of VLES by utilizing a semiclassical model with the CP softened by different parameters. The calculated two-dimensional (2D) electron momentum distributions and initial tunnel ionization time distributions exhibit that the VLES and HLES have different sensibilities to the variation of the CP, indicating that the influences of the CP on the two structures are different, which is further verified as being related, given the distance of the electron–parent ion Coulomb interaction. The formation and the underlying physical mechanism of the VLES are further identified by the initial tunnel ionization times of electrons with different final longitudinal momenta.

2. Theoretical methods

We calculate the low-energy ATI spectrum with the help of a semiclassical approach as employed in Refs. [35]–[38]. We consider a xenon atom ($I_p = 0.446$ a.u.) interacting with short laser pulses with a central wavelength $\lambda = 2000$ nm ($\omega = 0.0228$ a.u.) and an intensity $I = 8 \times 10^{13}$ W/cm^2, leading to a Keldysh parameter $\gamma = 0.45$, which is small enough for the ionization dynamics to be in the deep tunneling regime, such that the semiclassical picture can be verified.[35–38] We also consider that a xenon atom has a hydrogen-like potential of $V = -Z_{\rm eff}/r$ (where $Z_{\rm eff}$ is the effective nuclear charge to give ground state energy equal to that of a xenon atom).

In our calculation, the laser field $F(t)$ has a constant amplitude for the first ten cycles and then turns off within three cycles. It can be expressed as

$$F(t) = a(t)F_0 \cos \omega t, \tag{1}$$

where F_0 is the amplitude and the envelope function $a(t)$ is defined by

$$a(t) = \begin{cases} 1, & t \le 10T; \\ \cos^2 \dfrac{(t-10T)\pi}{6T}, & 10T < t \le 13T; \\ 0, & t > 13T, \end{cases} \tag{2}$$

where T is the laser pulse optical cycle. Note that the rising edge of the laser field envelope is not considered here, which can be justified as the ionization probability of the electron is exponentially proportional to the laser field amplitude and the ionization events mainly come from the peak of the laser field amplitude.

The ionization of electrons from a bound state to a continuum is described by a quantum tunneling ionization theory, i.e., electrons tunnel through a potential barrier created by the superposition of an atomic CP and a laser electric field with a probability given by the Ammosov–Delone–Krainov (ADK) formula.[39] The subsequent evolution of the ionized electron is described by a classical Newtonian equation

$$\frac{{\rm d}^2 \boldsymbol{r}}{{\rm d}t^2} = \boldsymbol{E}(t) + \nabla V, \tag{3}$$

where $\boldsymbol{E}(t) = (0, 0, F(t))$ is the linearly polarized electric field and $F(t)$ is given by Eq. (1).

In order to solve Eq. (3), the initial conditions, i.e., the initial position and velocity of the ionized electron need to be given. The initial position of the electron can be obtained from the tunnel ionization theory. In order to calculate the initial electron position, one can express the Schrödinger equation for a hydrogen-like atom in a uniform field ε in parabolic coordinates[39,40] as

$$\frac{{\rm d}^2\phi}{{\rm d}\eta^2} + \left(-\frac{I_p}{2} + \frac{1}{2\eta} + \frac{1}{4\eta^2} + \frac{1}{4}\varepsilon\eta\right)\phi = 0. \tag{4}$$

The above equation has the form of a one-dimensional (1D) Schrödinger equation with the potential

$$U(\eta) = -\left(\frac{1}{4\eta} + \frac{1}{8\eta^2} + \frac{1}{8}\varepsilon\eta\right)$$

and the energy $K = -I_p/4$ with I_p being the ionization potential of the atom. Thus, the outer turning point η_0 of the potential $U(\eta)$, viz., the "tunnel exit", where the electron becomes free, can be determined by $U(\eta) = K$. The initial positions of the tunnel ionized electron in the Cartesian coordinates can be obtained by $x_0 = y_0 = 0$ and $z_0 = -(1/2)\eta_0$.[35–38] In the quasistatic approximation, the above field parameter ε is related to the laser field amplitude $F(t)$ by $\varepsilon = F(t_0)$. The motion of

the electron is restricted in the plane (x, z) since the system is azimuthally symmetric about the polarization axis. The initial velocity is set to be $\upsilon_z = 0$ and $\upsilon_x = \upsilon_{x0}$. The weight of each trajectory is evaluated by[39]

$$w(t_0, \upsilon_{x0}) = w(0)\overline{w(1)}, \quad w(0) = \frac{4}{\varepsilon}\exp(-2/3\varepsilon),$$
$$\overline{w(1)} = \frac{\upsilon_{x0}}{\varepsilon\pi}\exp(-\upsilon_{x0}^2/\varepsilon). \tag{5}$$

In our calculations, 1×10^7 initial points are randomly distributed in the time interval $-\pi/2 \le \omega t \le \pi/2$ for the electrons that are tunnel ionized with a probability given by Delone and Krainov.[40] A set of trajectories are launched to simulate the behavior of the electron wave packet. An adaptive time step-size of 1 a.u. is applied in our calculations. In order to compare the results directly with the experimental data, which were obtained by a detector with a small solid angle with respect to the laser polarization,[20] we select only those electrons that are emitted along the field direction.

3. Results and discussion

The bottom curve in Fig. 1 shows the calculated result using the model described above, with the CP fully considered. One finds in the curve that an evident VLES is present at an electron energy < 0.5 eV, followed by a broader HLES with a high energy boundary of approximately 4.7 eV, in qualitative consistence with the experimental observation in Refs. [20] and [31]. If the CP is totally neglected after ionization, both the VLES and HLES completely disappear (top curve, Fig. 1). This is consistent with the simple-man model, in which the photoelectron spectrum below $2U_p$ is predicted to decrease exponentially from the origin. Therefore, we deduce that both the VLES and HLES are due to the effect of the CP. Similar conclusions have also been revealed in previous studies.[20,31]

In order to further understand how the Coulomb potential affects the VLES and HLES, we investigate the evolutions of these two structures with CP which is softened as $V = -Z_{\text{eff}}/\sqrt{a^2 + r^2}$, where a is a softening parameter used to adjust the depth of the potential and its attraction on the tunneled electrons. Note that when the CP is softened, the electrons far from the core are less influenced by the variation of the attractions than those close to the core. The relation between the attraction of the CP and the position of electrons is verified by Huang *et al.*[41] who compared the influences of the CP on the transverse momentum by employing a short or a long-range potential in their calculations. The middle curve in Fig. 1 displays the results obtained by softening the CP with a parameter of 10. The high energy boundary of the HLES decreases to approximately 4.1 eV, indicating that the change in CP may cause a shift of the highest energy of the LES. More importantly, the VLES becomes smooth and even invisible, whereas the HLES is still clearly visible, although it is not so pronounced as that of the pure CP (i.e., with a softening parameter $a = 0$), revealing that the appearance of the VLES is more sensitive to the change of the Coulomb attraction than that of the HLES. Thus, although the two structures are generally considered to be due to the CP,[20,31,32] they feel different influences from the CP since the electrons, contributing to the two structures, interact with the core at different distances, which we will look more closely at in the remaining part of the paper.

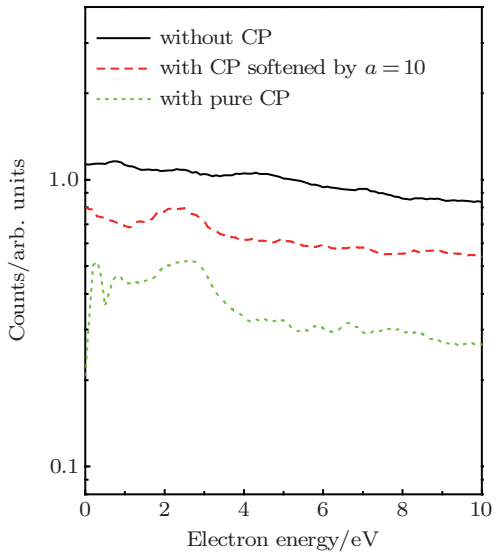


Fig. 1. (color online) Photoelectron spectra of xenon, obtained by semi-classical calculations in the cases without CP, with CP softened by a parameter of 10 and with pure CP for the curves from top to bottom, respectively. $I = 8\times10^{13}$ W/cm^2 and $\lambda = 2000$ nm. The curves are shifted vertically for visual convenience.

In order to understand in more detail the origin of the VLES, we calculate the density plot of the 2D electron momentum distributions for two types of electron trajectories, i.e., direct electrons and indirect ones, depending on their initial tunnel ionization times as adopted in Ref. [20]. According to the simple-man theory, the direct electrons are tunnel ionized on the rising edge of the laser field, i.e., $\omega t \in [-\pi/2, 0]$; they are then driven by the field and move away. The indirect electrons are tunnel ionized on the falling edge of the laser field, i.e., $\omega t \in [0, \pi/2]$, which then oscillate in the laser field. These electrons may return and collide with the core and then absorb enough energy to escape. Note that these two types of electron trajectories originate from the description of the simple-man theory, which neglects the effect of the CP on the tunneled electron. In our study, however, the tunneled electrons evolve in the combined CP and the laser fields.

The calculated 2D electron momentum distributions at $I = 8\times10^{13}$ W/cm^2 and $\lambda = 2000$ nm are presented in Fig. 2. The

momentum along the polarization direction of the linearly polarized laser is termed P_z, while P_x corresponds to the momentum perpendicular to the polarization direction. Figures 2(a) and 2(d) display the calculated momentum distributions for electrons initially tunnel ionized on the rising and falling edges of the laser field, respectively, with the CP neglected. Most electrons are evidently distributed around zero momentum; the distributions become sparse as the momentum increases. The direct and indirect electrons are symmetrically distributed with respect to P_x. Apparently, the corresponding energy spectrum, obtained by projecting the momentum distribution onto the P_z axis, exhibits no structures, which is in accordance with the top curve shown in Fig. 1. The features of these distributions are in good agreement with the prediction of the simple-man model.

For comparison, the momentum distributions calculated by taking into account a pure CP are displayed in Figs. 2(b) and 2(e) for electrons ionized on the rising and falling edges of the laser field, respectively. Remarkably, the momentum distributions along the P_x axis are still symmetrical but the overall momentum distributions are changed by the CP; some peculiar features emerge. One feature is that, with a pure CP considered [Fig. 2(b)], the overall momentum distributions shift along the P_z axis with a positive value of 0.19 a.u., in contrast to the fact that all momenta of direct electrons are distributed below zero when the CP is neglected [Fig. 2(a)]. This value of 0.19 a.u corresponds to a kinetic energy of 0.5 eV, which equals the high energy boundary of VLES in the energy spectra [see Fig. 1]. Moreover, Fig. 2(b) shows that a visible small accumulation area appears for the electrons ionized on the rising edge. The central part of this area is around 0.13 a.u., corresponding to a kinetic energy of 0.23 eV, which is approximately the center of VLES in the energy spectra. Figure 2(b) also shows that the electrons are distributed closer to the P_z axis than those in Fig. 2(a), i.e., the overall momentum distributions become significantly narrow when a pure CP is considered. On the other hand, the CP manifests a similar effect on electrons ionized on the falling edge of the laser field, i.e., indirect electrons. Figure 2(e) shows that the indirect electrons are mainly distributed in two different small accumulation areas. One area is close to zero while its central position in the energy spectrum is higher than that of the VLES but lower than that of the HLES, almost between the two structures; it is, however, less resolvable in the data. The other area is located in a higher momentum area and its central position is approximately 0.42 a.u. The momentum of 0.42 a.u. corresponds to a kinetic energy of 2.4 eV, which is approximately the central position of the HLES. The width of this area is much broader in the direction of the field, leading to a broad HLES appearing in the energy spectrum.

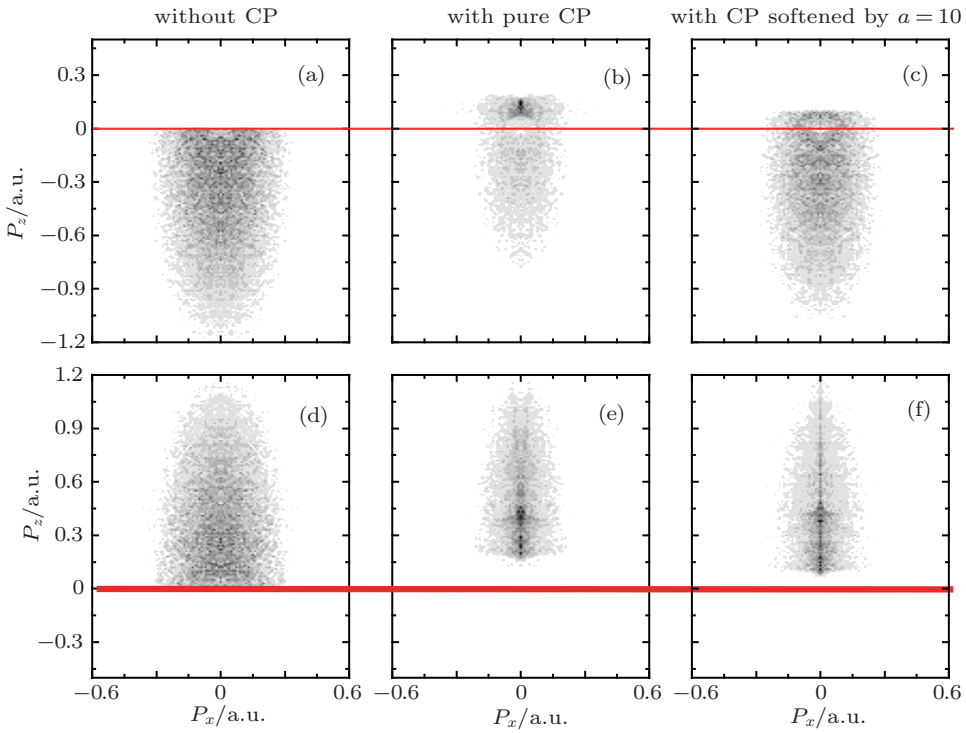


Fig. 2. (color online) Calculated momentum distributions for electrons tunnel ionized on the rising edge [(a)–(c)] and the falling edge [(d)–(f)] of the laser electric field. (a), (d) without CP; (b), (e) with pure CP; and (e), (d) with CP softened by a parameter of 10. The laser polarization direction is along the z axis and the red horizontal lines indicate that $P_z = 0$. The laser parameters are the same as those in Fig. 1. For more details, see text.

In order to elucidate the evolution of VLES with CP, we further calculate the electron momentum distributions by softening the CP with a parameter of 10 [Figs. 2(c) and 2(f)]. Obviously, figure 2(c) shows that the electrons ionized on the rising edge exhibit less of a momentum shift than that in Fig. 2(b), which can be expected since the attraction from CP is reduced by the softening parameter. It is noteworthy that in this case, the accumulation area, which is pronounced for a pure CP (see Fig. 2(b)), almost disappears; the momenta are uniformly distributed along the P_z axis, although the overall momentum distribution is narrower than that in Fig. 2(a). However, the top boundary of the direct electron is below the low boundary of the VLES (about 0.1 a.u.), which means that the electrons in the momentum regime corresponding to VLES (0.1 a.u.–0.2 a.u.) are indirect electrons on the falling edge of the electric field. On the other hand, for the electrons ionized on the falling edge of the laser field [Fig. 2(f)], the accumulation areas, which now correspond to both the HLES and the VLES in the energy spectrum, still exist although these areas become less evident. As shown in Fig. 1, the HLES is still apparent but the VLES is hardly distinguished, indicating that the HLES is less sensitive to the softening of CP than the VLES. Moreover, a closer comparison of Fig. 2(f) with Fig. 2(d) shows that the overall momentum distribution of the electrons ionized on the falling edge is still concentrated along the P_z axis even when the CP is softened, in contrast to direct electrons (Fig. 2(c)). This clearly indicates that the softening of CP has less of an effect on the indirect electrons than on the direct electrons.

From the viewpoint of the simple-man picture, the shift of the overall momentum distribution in the field direction can be understood as that besides the interaction with the laser field, the electrons also feel additional attractive force of the CP when they leave the saddle point after tunneling. This force exists and plays the same role in changing the wave packet's longitudinal momentum of the electrons ionized on both the rising and falling edges, leading to the electrons shifting in the same direction and the overall momentum distribution shifting in the positive direction of the field direction.

On the other hand, the evolutions of both the energy spectrum and the momentum distribution with the softened parameter exhibit that the VLES is more sensitive to the variation of the CP than the HLES. The electrons contributing to the HLES are indirect electrons ionized at the laser phases away from the maximum of the field. They may return to the core with higher kinetic energies and pass through the core multiple times.[20,26] The lower sensitivity of the HLES to the change of the CP reveals that these electrons interact with the parent ions at a large distance from the core, thus they are still significantly affected though the CP is softened. In contrast, the electrons contributing to VLES are more sensitive to the variation of the CP, indicating that they are born in a regime much closer to the parent ion core and interact with it at a small distance. Therefore, the accumulation area in Fig. 2(f) is less visible and the VLES is hardly distinguished when the CP is softened (see Fig. 1). This is consistent with the result of Refs. [31] and [32] that the VLES is mainly contributed by the electrons ionized very near the peak of the field, which will be driven back to the core with very low kinetic energy and interact with the ionic potential strongly at a short distance. Therefore, the VLES can be attributed to the interaction of the tunneled electrons with the parent ion core at a distance much closer to the ion, while the HLES can be attributed to that at a larger distance.

Furthermore, we collect all electron trajectories with final energies falling in the VLES regime (i.e., < 0.45 eV) and plot in Fig. 3 the distributions of the laser phases corresponding to their initial tunnel ionization times. Without considering the CP, the tunneling times are confined in two regions, one is on the rising edge and the other on the falling edge [see Fig. 3(a)]. The two regions are symmetric with respect to the origin: the central positions of the left and right regions are –4° and +4°, respectively. This symmetry is consistent with the simple-man prediction. In contrast, the distribution of the tunneling times with a pure CP [see Fig. 3(c)] shows that the symmetry breaks down due to the shift induced by the CP and most electrons are emitted on the rising edge, i.e., the contribution is mainly from the direct electron.

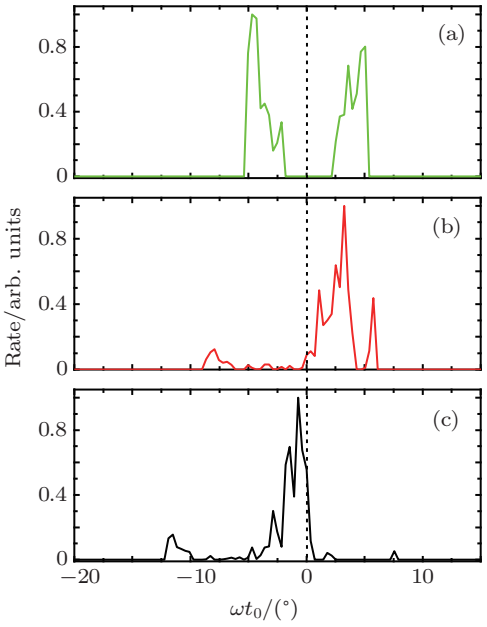


Fig. 3. (color online) Normalized distributions of the initial tunnel ionization phase (ωt_0) of electrons with final energies in the VLES regime (i.e., electron energy ≤ 0.45 eV for the lowest curve in Fig. 1), in the cases without CP (a), with CP softened by a parameter of 10 (b) and with pure CP (c). The black vertical dot line indicates the position of $\omega t_0 = 0$ for visual convenience.

In contrast, the distribution of the tunneling times with CP softened by a parameter of 10 [Fig. 3(b)] shows that the

tunneling times are still almost confined in the right region, which corresponds to the indirect electrons. This is well consistent with the case in Fig. 2 and the above analyses.

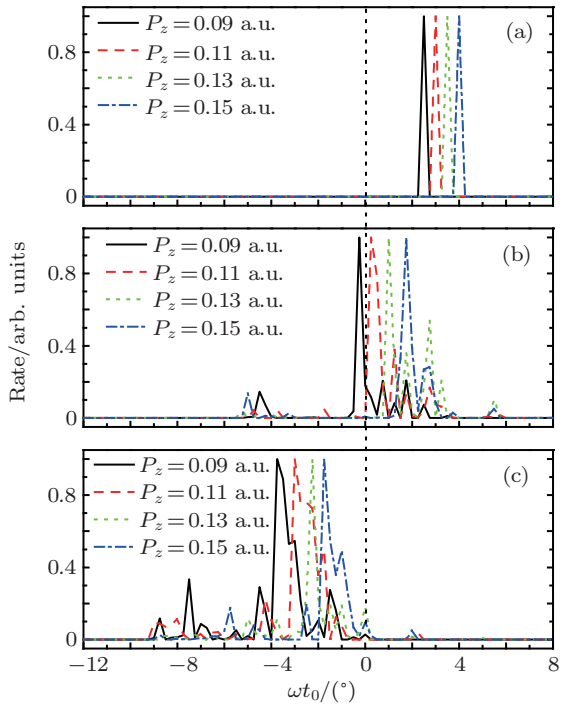


Fig. 4. (color online) Normalized distributions of the initial tunnel ionization phase (ωt_0) of electrons with the corresponding final longitudinal momenta in the field direction (P_z) for the cases without CP (a), with CP softened by a parameter of 10 (b) and with pure CP (c). The vertical dot line indicates the position of $\omega t_0 = 0$ for visual convenience.

To further explore the effect of the change of the CP on the VLES, we track the initial tunnel ionization phase (ωt_0) of the electrons with different final longitudinal momenta in the field direction (Fig. 4). The final longitudinal momenta range from 0.09 a.u. to 0.15 a.u., which is located in the VLES regime. At first glance, figure 4(a)–4(c) show that the phase is gradually shifted to the left as the CP is gradually strengthened, which is in accordance with the case in Fig. 3. On closer inspection, when the CP is totally neglected [Fig. 4(a)], the phases of different final drift momenta are well separated and increase with momentum increasing, which is consistent with the simple-man prediction, in which the final longitudinal momentum is solely determined by the laser phase when the electron tunnels out. However, when a pure CP is included [Fig. 4(c)], although the phase still increases with the increasing of momentum, it is exhibited that a distinct overlap occurs for different longitudinal momenta; further, the average phase of the electron with P_z in the range from 0.09 a.u. to 0.15 a.u. is at approximately –2.5°, indicating that the phase is redistributed by the CP. The CP significantly distorts the trajectories of electrons under different initial conditions and bunches the final longitudinal momenta, resulting in an identical momentum, which corresponds to the accumulation area in Fig. 2(b). Moreover, when the CP is softened by a parameter of 10 [Fig. 4(b)], the overlapping degree of the phases of different momenta is smaller than that with a pure CP, revealing that a bunching of the final longitudinal momenta becomes weak. This explains that though the accumulation area corresponding to VLES can still be seen in the momentum distribution (see Fig. 2(f)), the VLES fades out and can be hardly distinguished in the energy spectrum (see Fig. 1). Therefore, we provide an additional sound evidence that the formation of the VLES is due to an energy-bunching effect of the CP on the low-energy electrons and this bunching effect is strongly dependent on the strength of the attract potential.

4. Conclusions

In this paper, we performed semiclassical calculations of both energy spectra and 2D momentum distributions of the low-energy electrons of xenon atom ionized in a mid-infrared laser field. Our analysis shows that the VLES is more sensitive to the changes of the CP than the HLES and the VLES is identified as originating from the interaction of the tunneled electron with the parent ion core at a small distance, while the HLES is attributed to that at a large distance. The distributions of the initial tunnel ionization phase directly verify that the formation of the VLES is due to the energy-bunching of the low-energy electrons by the CP.

References

[1] Agostini P, Fabre F, Mainfray G, Petite G and Rahman N K 1979 *Phys. Rev. Lett.* **42** 1127
[2] DiMauro L F and Agostini P 1995 *Adv. At. Mol. Opt. Phys.* **35** 79
[3] Becker W, Grasbon F, Kopold R, Milošević D B, Paulus G G and Walther H 2002 *Adv. At. Mol. Opt. Phys.* **48** 35
[4] Milošević D B and Ehlotzky F 2003 *Adv. At. Mol. Opt. Phys.* **49** 373
[5] Agostini P and DiMauro L F 2008 *Contemp. Phys.* **49** 179
[6] Keldysh L V 1965 *Sov. Phys. JETP* **20** 1307
[7] Bucksbaum P H, Freeman R R, Bashkansky M and Mcilrath T J 1987 *J. Opt. Soc. Am. B* **4** 760
[8] Corkum P B, Burnett N H and Brunel F 1989 *Phys. Rev. Lett.* **62** 1259
[9] Corkum P B 1993 *Phys. Rev. Lett.* **71** 1994
[10] Schafer K J, Yang B R, DiMauro L F and Kulander K C 1993 *Phys. Rev. Lett.* **70** 1599
[11] Paulus G G, Becker W, Nicklich W and Walther H 1994 *J. Phys. B: At. Mol. Opt. Phys.* **27** L703
[12] Paulus G G, Nicklich W, Xu H L, Lambropoulos P and Walther H 1994 *Phys. Rev. Lett.* **72** 2851
[13] Yang B R, Schafer K J, Walker B, Kulander K C, Agostini P and DiMauro L F 1993 *Phys. Rev. Lett.* **71** 3770
[14] Colosimo P, Doumy G, Blaga C I, Wheeler J, Hauri C, Catoire F, Tate J, Chirla R, March A M, Paulus G G, Muller H G, Agostini P and DiMauro L F 2008 *Nat. Phys.* **4** 386
[15] Chen J and Nam C H 2002 *Phys. Rev. A* **66** 053415
[16] Moshammer R, Ullrich J, Feuerstein B, Fischer D, Dorn A, Schröter C D, Crespo L-U J R, Hoehr C, Rottke H, Trump C, Wittmann M, Korn G and Sandner W 2003 *Phys. Rev. Lett.* **91** 113002
[17] Rudenko A K, Zrost K, Schröter C D, de Jesus V L B, Feuerstein B, Moshammer R and Ullrich J 2004 *J. Phys. B: At. Mol. Opt. Phys.* **37** L407
[18] Alnaser A S, Maharjan C M, Wang P and Litvinyuk I V 2006 *J. Phys. B: At. Mol. Opt. Phys.* **39** L323
[19] Blaga C I, Catoire F, Colosimo P, Paulus G G, Muller H G, Agostini P and DiMauro L F 2009 *Nat. Phys.* **5** 335

[20] Quan W, Lin Z, Wu M, Kang H, Liu H, Liu X, Chen J, Liu J, He X T, Chen S G, Xiong H, Guo L, Xu H, Fu Y, Cheng Y and Xu Z Z 2009 *Phys. Rev. Lett.* **103** 093001
[21] Faisal H M 2009 *Nat. Phys.* **5** 319
[22] Catoire F, Blaga C I, Sistrunk E, Muller H G, Agostini P and DiMauro L 2009 *Laser Phys.* **19** 1574
[23] Chu W, Wu M Y, Zeng B, Yao J P, Ni J L, Xiong H, Xu H, Lin Z Y, Kang H P, Quan W, Chen J, Liu X, Cheng Y and Xu Z Z 2012 *Phys. Rev. A* **85** 021403(R)
[24] Faisal F H 1973 *J. Phys. B: At. Mol. Opt. Phys.* **6** L89
[25] Reiss H R 1980 *Phys. Rev. A* **22** 1786
[26] Liu C P and Hatsagortsyan K Z 2010 *Phys. Rev. Lett.* **105** 113003
[27] Liu C P and Hatsagortsyan K Z 2011 *J. Phys. B: At. Mol. Opt. Phys.* **44** 095402
[28] Yan T M, Popruzhenko S V, Vrakking M J J and Bauer D 2010 *Phys. Rev. Lett.* **105** 253002
[29] Lemell C, Dimitriou K I, Tong X M, Nagele S, Kartashov D V, Burgdörfer J and Gräfe S 2012 *Phys. Rev. A* **85** 011403(R)
[30] Guo L, Han S S, Liu X, Cheng Y, Xu Z Z, Fan J, Chen J, Chen S G, Becker W, Blaga C I, DiChiara A D, Sistrunk E, Agostini P and DiMauro L F 2013 *Phys. Rev. Lett.* **110** 013001
[31] Wu C Y, Yang Y D, Liu Y Q, Gong Q H, Wu M, Liu X, Hao X L, Li W D, He X T and Chen J 2012 *Phys. Rev. Lett.* **109** 043001
[32] Kästner A, Saalmann U and Rost J M 2012 *Phys. Rev. Lett.* **108** 033201
[33] Lemell C, Burgdörfer J, Gräfe S, Dimitriou K I, Arbó D G and Tong X M 2013 *Phys. Rev. A* **87** 013421
[34] Agostini P and DiMauro L F 2012 *Adv. At. Mol. Opt. Phys.* **61** 118
[35] Hu B, Liu J and Chen S G 1997 *Phys. Lett. A* **236** 533
[36] Chen J, Liu J and Zheng W M 2002 *Phys. Rev. A* **66** 043410
[37] Ye D F, Liu X and Liu J 2008 *Phys. Rev. Lett.* **101** 233003
[38] Hao X L, Li W D, Liu J and Chen J 2012 *Chin. Phys. B* **21** 083304
[39] Delone N B and Krainov V P 1991 *J. Opt. Soc. Am. B* **8** 1207
[40] Landau L D and Lifshitz E M 1977 *Quantum Mechanics* (New York: Pergamon)
[41] Huang C, Liao Q, Zhou Y M and Lu P X 2010 *Opt. Express* **18** 14293